

Multi-organ assessment in mainly non-hospitalized individuals after SARS-CoV-2 infection: The Hamburg City Health Study COVID programme

Elina Larissa Petersen ^{1,2}, Alina Goßling ^{1,2}, Gerhard Adam³,
Martin Aepfelbacher⁴, Christian-Alexander Behrendt ^{1,2}, Ersin Cavus^{1,2,5},
Bastian Cheng ⁶, Nicole Fischer ⁴, Jürgen Gallinat⁷, Simone Kühn⁷,
Christian Gerloff⁶, Uwe Koch-Gromus⁸, Martin Härter⁸, Uta Hanning^{3,9},
Tobias B. Huber ¹⁰, Stefan Kluge ¹¹, Johannes K. Knobloch ⁴, Piotr Kuta¹²,
Christian Schmidt-Lauber¹⁰, Marc Lütgehetmann ⁴, Christina Magnussen ^{1,2,5},
Carola Mayer ⁶, Kai Muellerleile^{1,2,5}, Julia Münch ^{1,2}, Felix Leonard Nägele ⁶,
Marvin Petersen ⁶, Thomas Renné ^{12,13,14}, Katharina Alina Riedl ^{1,2},
David Leander Rimmel ⁶, Ines Schäfer^{1,2}, Holger Schulz ⁸, Enver Tahir ³,
Benjamin Waschki^{1,5,15,16}, Jan-Per Wenzel ^{1,2}, Tanja Zeller^{5,17},
Andreas Ziegler ^{1,18,19}, Götz Thomalla ^{6†}, Raphael Twerenbold ^{1,2,5,17†}, and
Stefan Blankenberg^{1,2,5*†}

¹Department of Cardiology, University Heart and Vascular Center, Hamburg, Germany; ²Population Health Research Department, University Heart and Vascular Center, Hamburg, Germany; ³Department of Diagnostic and Interventional Radiology and Nuclear Medicine, University Medical Center Hamburg-Eppendorf, Hamburg, Germany; ⁴Institute of Medical Microbiology, Virology and Hygiene, University Medical Center Hamburg-Eppendorf, Hamburg, Germany; ⁵German Center for Cardiovascular Research (DZHK), partner site Hamburg/Kiel/Luebeck, Hamburg, Germany; ⁶Department of Neurology, University Medical Center Hamburg-Eppendorf, Hamburg, Germany; ⁷Clinic and Policlinic for Psychiatry and Psychotherapy, University Clinic Hamburg-Eppendorf, Hamburg, Germany; ⁸Department of Medical Psychology, University Medical Center Hamburg-Eppendorf (UKE), Hamburg, Germany; ⁹Department of Diagnostic and Interventional Neuroradiology, University Medical Center Hamburg-Eppendorf, Hamburg, Germany; ¹⁰III. Department of Medicine, University Medical Center Hamburg-Eppendorf, Hamburg, Germany; ¹¹Department of Intensive Care Medicine, University Medical Center Hamburg-Eppendorf, Hamburg, Germany; ¹²Institute of Clinical Chemistry and Laboratory Medicine, University Medical Center Hamburg-Eppendorf, Hamburg, Germany; ¹³Center for Thrombosis and Hemostasis (CTH), Johannes Gutenberg University Medical Center, Mainz, Germany; ¹⁴Irish Centre for Vascular Biology, School of Pharmacy and Biomolecular Sciences, Royal College of Surgeons in Ireland, Dublin, Ireland; ¹⁵Hospital Itzehoe, Pneumology, Itzehoe, Germany; ¹⁶Airway Research Center North (ARCN), German Center for Lung Research (DZL), LungenClinic Grosshansdorf, Grosshansdorf, Germany; ¹⁷University Center of Cardiovascular Science, University Heart and Vascular Center, Hamburg, Germany; ¹⁸Cardio-CARE, Medizincampus Davos, Davos, Switzerland; and ¹⁹School of Mathematics, Statistics and Computer Science, University of KwaZulu-Natal, Pietermaritzburg, South Africa

Received 6 October 2021; revised 24 December 2021; accepted 25 December 2021; online publish-ahead-of-print 6 January 2022

See the editorial comment for this article 'Post-COVID-19 illness trajectory in community patients: mostly reassuring results', by Colin Berry and Hannah K. Bayes, <https://doi.org/10.1093/eurheartj/ehac057>.

Aims

Long-term sequelae may occur after SARS-CoV-2 infection. We comprehensively assessed organ-specific functions in individuals after mild to moderate SARS-CoV-2 infection compared with controls from the general population.

* Corresponding author. Tel: +49 40 7410 53972/56800, Fax: +49 40 7410 53622, Email: s.blankenberg@uke.de

† These authors contributed equally.

© The Author(s) 2022. Published by Oxford University Press on behalf of European Society of Cardiology.

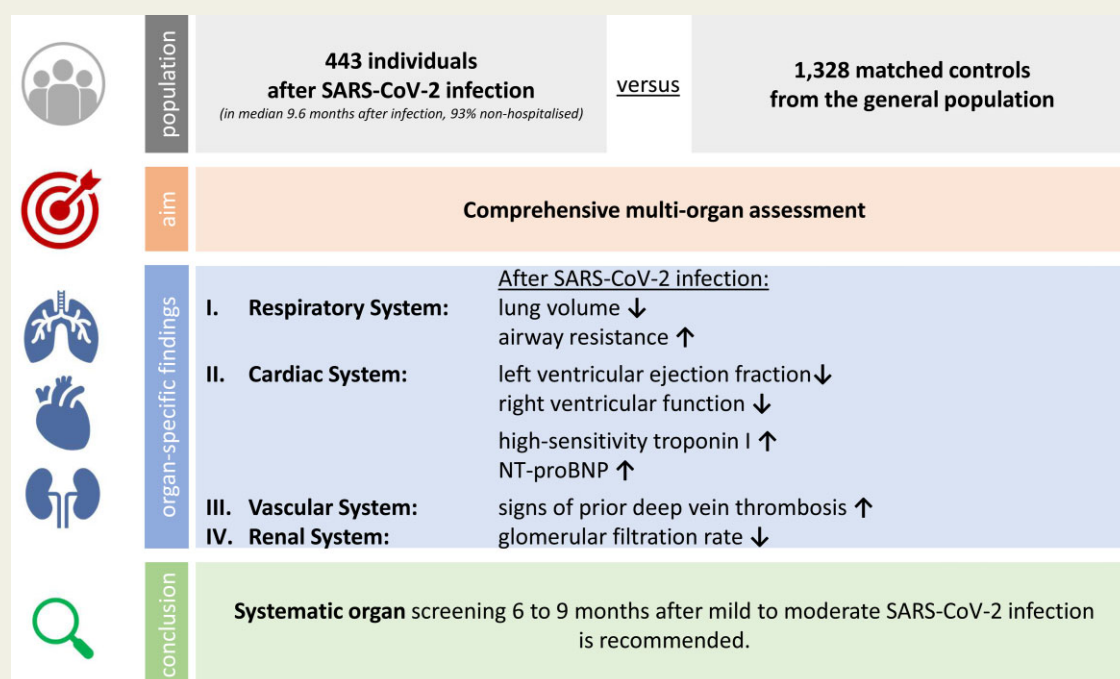
This is an Open Access article distributed under the terms of the Creative Commons Attribution Non-Commercial License (<http://creativecommons.org/licenses/by-nc/4.0/>), which permits non-commercial re-use, distribution, and reproduction in any medium, provided the original work is properly cited. For commercial re-use, please contact journals.permissions@oup.com

Methods and results

Four hundred and forty-three mainly non-hospitalized individuals were examined in median 9.6 months after the first positive SARS-CoV-2 test and matched for age, sex, and education with 1328 controls from a population-based German cohort. We assessed pulmonary, cardiac, vascular, renal, and neurological status, as well as patient-related outcomes. Bodyplethysmography documented mildly lower total lung volume (regression coefficient -3.24 , adjusted $P=0.014$) and higher specific airway resistance (regression coefficient 8.11 , adjusted $P=0.001$) after SARS-CoV-2 infection. Cardiac assessment revealed slightly lower measures of left (regression coefficient for left ventricular ejection fraction on transthoracic echocardiography -0.93 , adjusted $P=0.015$) and right ventricular function and higher concentrations of cardiac biomarkers (factor 1.14 for high-sensitivity troponin, 1.41 for N-terminal pro-B-type natriuretic peptide, adjusted $P \leq 0.01$) in post-SARS-CoV-2 patients compared with matched controls, but no significant differences in cardiac magnetic resonance imaging findings. Sonographically non-compressible femoral veins, suggesting deep vein thrombosis, were substantially more frequent after SARS-CoV-2 infection (odds ratio 2.68 , adjusted $P < 0.001$). Glomerular filtration rate (regression coefficient -2.35 , adjusted $P=0.019$) was lower in post-SARS-CoV-2 cases. Relative brain volume, prevalence of cerebral microbleeds, and infarct residuals were similar, while the mean cortical thickness was higher in post-SARS-CoV-2 cases. Cognitive function was not impaired. Similarly, patient-related outcomes did not differ.

Conclusion

Subjects who apparently recovered from mild to moderate SARS-CoV-2 infection show signs of subclinical multi-organ affection related to pulmonary, cardiac, thrombotic, and renal function without signs of structural brain damage, neurocognitive, or quality-of-life impairment. Respective screening may guide further patient management.



Graphical Abstract The key question is: How does a mild to moderate course of SARS-CoV-2 infection in mainly non-hospitalized individuals impact intermediate-term organ-specific functions in comparison to the general population? The key findings are (i) a mild to moderate course of SARS-CoV-2 infection is associated with subsequent signs of subclinical multi-organ affection; (ii) associations mainly affect the pulmonary, cardiac, coagulation, and renal system; and (iii) no systematic associations with structural brain damage, neurocognition, or quality of life were observed. The take-home message is systematic screening of multi-organ function even after mild to moderate SARS-CoV-2 infection is recommended to identify individuals at risk and initiate appropriate preventive therapies.

Keywords

COVID-19 • Sequelae • Matched controls • Multi-organ assessment

Introduction

As of December 2021, the coronavirus disease 2019 (COVID-19) pandemic has resulted in over 260 million confirmed positive

cases of severe acute respiratory syndrome coronavirus type 2 (SARS-CoV-2) globally.¹ In Europe, 3.6% of infected patients required intensive care, 90% recovered in an ambulatory setting.^{2,3}

Severe COVID-19 may affect multiple organ systems during the acute phase of the disease. The impairment of pulmonary, cardiac, and renal function as well as thromboembolism have been described in severely ill and deceased patients.^{4–6} Furthermore, serious neurological complications, including cerebrovascular events, encephalopathy, and encephalitis, have been reported.⁷

While single reports describe persisting symptoms of pulmonary, renal, cardiac, or vascular dysfunction as well as fatigue or depression mostly derived from hospitalized cohorts,⁸ a systematic investigation especially of subclinical changes of multi-organ structure and function is of particular interest in the current pandemic context.

With this study, we aimed to comprehensively determine the intermediate-term impact of a mild to moderate course of COVID-19 on organ-specific function. A COVID-19 disease course was classified as mild to moderate when not requiring intensive care unit treatment. We assessed multi-organ function by deep phenotyping in patients ~9 months after COVID-19 recovery in direct comparison with age-, sex-, and education-matched subjects from a population-based cohort study.

Methods

Study design

We report a cross-sectional study to compare the organ-specific functions and structures assessed in a cohort of subjects with prior mild to moderate SARS-CoV-2 infection with matched subjects from an ongoing, prospective, population-based cohort study.

Study population

The post-SARS-CoV-2 cohort consists of subjects living in the metropolitan area of Hamburg, Germany, with a laboratory-confirmed positive polymerase chain reaction (PCR) test for SARS-CoV-2, obtained between 1 March and 31 December 2020 at least 4 months prior to study enrollment. In correspondence to the age structure of the population-based Hamburg City Health Study (HCHS), which served as the control cohort, participants had to be 45–74 years old at the time of recruitment.⁹

Eligible participants after SARS-CoV-2 infection were invited to participate after they were automatically identified through the clinical information system of the University Medical Center Hamburg-Eppendorf (UKE), which performed SARS-CoV-2 diagnostics for the public health service. In addition, eligible inhabitants living in the metropolitan area were invited to participate via public announcement. At the time of study enrollment, all participants provided written informed consent. The local ethics committee (State of Hamburg Chamber of Medical Practitioners, PV5131) did not have objections against the recruitment of post-SARS-CoV-2 individuals and the study protocol as an extension of the HCHS, and the study was conducted in compliance with the Declaration of Helsinki. Categorization of disease severity was based on retrospectively documented, self-reported symptom severity at the time of SARS-CoV-2 infection and consisted of four groups: asymptomatic, mild symptoms, moderate symptoms without the need for hospitalization, and moderate symptoms with the need for hospitalization.

Matched controls were selected from the HCHS (ClinicalTrials.gov identifier NCT03934957), a large, ongoing, prospective, population-based cohort study conducted at the University Medical Center Hamburg-Eppendorf (UKE), Germany, since 2016 to gain knowledge

about major chronic diseases.⁹ As of July 2021, data from ~15 000 participants were available.

Hamburg City Health Study participants were only eligible as controls for this work if they had been enrolled prior to being at risk of infection with SARS-CoV-2 and during the same seasonal period as the patients after SARS-CoV-2 infection. The inclusion periods were November–April 2016–19.

Outcomes and data collection

Both patients after SARS-CoV-2 infection and matched controls underwent the same standardized 7 h assessment at the Epidemiological Study Center of the Population Health Research Department of the University Medical Center Hamburg-Eppendorf (UKE), which has been described elsewhere.⁹

Pulmonary phenotyping

Lung function was assessed by trained technicians performing bodyplethysmography including forced spirometry (MasterScreen with SentrySuite, Vyaire Medical GmbH, Hoechberg, Germany) according to international guidelines.^{10,11} Forced spirometry manoeuvres were performed to obtain forced expiratory volume in 1 s (FEV₁) and forced vital capacity (FVC). Resistance manoeuvres were performed a minimum of five times, all other manoeuvres were performed a minimum of three times. Bodyplethysmography was conducted to obtain the specific airway resistance (sRaw) and static lung volumes. Lung volumes were obtained by means of functional residual capacity (FRC) measured during gentle breathing against a shutter as well as expiratory reserve volume and vital capacity (VC). Residual volume was calculated by subtracting expiratory reserve volume from FRC, and total lung capacity (TLC) was calculated by the addition of residual volume and VC. For quality control, a multidimensional quality assurance concept was established, including regular calibration of the equipment, regular training and certification of the technicians, and a combination of algorithm-based data processing and visual control by a trained examiner. We used FEV₁, the ratio of FEV₁ and FVC, and sRaw to assess airway function and FVC, VC, TLC, and FRC to assess lung volumes.

Cardiac phenotyping

Transthoracic echocardiography was performed and analysed by cardiologists and sonographers (technicians) (Siemens Acuson SC2000 Prime, Siemens Healthineers, Erlangen, Germany). Technical details on transthoracic echocardiography data collection and quality assurance have been described elsewhere.¹² Left ventricular ejection fraction was assessed using disks summation in two-dimensional (2D) and 3D loops. Mitral inflow pattern was assessed in the apical four-chamber view by placing pulsed-wave (PW) Doppler sample volume between mitral leaflet tips. Pulsed-wave tissue Doppler imaging (TDI) e' velocity was measured in the apical four-chamber view by placing the sample volume at the lateral and septal basal regions of the mitral annulus. To assess the left ventricular diastolic function, E/e' was computed as the mean ratio of E-wave velocity divided by e' lateral and septal velocity. The right ventricular longitudinal function was quantified by the systolic excursion of the tricuspid annulus. The tricuspid annular plane systolic excursion (TAPSE) was obtained by M-mode echocardiography in the apical four-chamber view, reflecting right ventricular ejection fraction. The peak tricuspid regurgitation velocity, representing right ventricular filling pressure, was measured in the apical four-chamber view by continuous-wave Doppler.

Cardiovascular magnetic resonance imaging (MRI) was performed on a 3 T scanner (MAGNETOM™ Skyra, Siemens Healthineers,

Erlangen, Germany). The protocol included standard electrocardiogram (ECG)-triggered steady-state free-precession cine series in short axis for biventricular estimation of ejection fraction using the commercially available software 'CVi42' (Circle Cardiovascular Imaging Inc., Calgary, Alberta, Canada). Endo- and epicardial borders of the left and right ventricles were manually delineated on short-axis cine images as recommended.^{13,14} Pre-contrast (native) T1 mapping was performed using a commercially available modified Look-Locker inversion recovery (MOLLI) sequence with a 5b(3b)3b scheme, T2 mapping using a T2-prepared single-shot fast low-angle shot (FLASH) sequence. The myocardium was automatically divided into 16 segments according to the American Heart Association (AHA) segment model and the mid-anteroseptal myocardial AHA segment VIII providing the most robust measurements of myocardial T1 and T2 and predominantly used to assess diffuse myocardial tissue alterations in clinical routine was selected for the analyses.¹⁵ Late gadolinium enhancement (LGE) imaging was performed (phase-sensitive inversion recovery, PSIR) in short-axis orientation covering the entire heart and in two-, three-, and four-chamber views. Late gadolinium enhancement was evaluated qualitatively.¹⁴

Electrocardiogram at rest was recorded with a standard digital 12-lead ECG (Schiller, Baar, Switzerland) and included a 2 min rhythm strip.

Vascular phenotyping

Study participants underwent a compression ultrasound of the left and right common femoral vein using a Siemens SC2000 with a 7.5 MHz linear probe (Siemens Healthcare GmbH, Erlangen, Germany). Trained technicians performed the ultrasound examination following a standard protocol, and a regular quality assurance of research data was conducted via statistical measures as well as random and risk-based controls by specialized physicians. A static grey-scale image (brightness mode) of the common femoral vein was captured at the level of the saphenofemoral junction both with and without external mechanical compression.

A vascular specialist reviewed images from all post-SARS-CoV-2 participants ($n = 443$) and from a random sample of the matched controls ($n = 400$). If the common femoral vein was not fully compressible, the corresponding image was independently reviewed by a second vascular specialist. Only in the case of agreement between both investigators, veins were declared non-compressible.

Carotid atherosclerosis and flow velocities were evaluated by ultrasound using a Siemens SC2000[®] with a 7.5 MHz linear array transducer. Measurements of ultrasound parameters were performed as reported previously.¹⁶ In brief, carotid intima-media thickness (CIMT) was measured three times in the B-mode in a longitudinal view of the left and right common carotid artery (CCA) >1 cm proximal to the carotid bulb, and mean values were calculated. The presence of atherosclerotic plaques was recorded. The peak systolic flow velocity (PSV) of the CCA and internal carotid artery (ICA) were measured by PW Doppler.

Neuroimaging phenotyping

Images were acquired using a 3 T scanner (MAGNETOM[™] Skyra, Siemens Healthineers, Erlangen, Germany). For 3D T1-weighted anatomical images, rapid acquisition gradient-echo sequence (MPRAGE) was used with the following sequence parameters: repetition time (TR) = 2500 ms, echo time (TE) = 2.12 ms, 256 axial slices, slice thickness (ST) = 0.94 mm, and in-plane resolution (IPR) = 0.83×0.83 mm². Three-dimensional T2-weighted fluid attenuated inversion recovery (FLAIR) images were acquired with the following sequence parameters: TR = 4700 ms, TE = 392 ms, 192 axial slices, ST = 0.9 mm, and IPR = 0.75×0.75 mm. Time of flight (TOF) magnetic resonance angiography was performed using TR = 25 ms, TE = 3.6 ms,

64 axial slices, ST = 0.5 mm, IPR = 0.7×0.7 mm, GRAPPA 2, flip angle (FA) = 25°, and bandwidth 133 Hz/Px positioned transversal over the circle of Willis.

Cortical thickness, brain volume, and intracranial volumes were quantified based on T1-weighted imaging data using the standardized FreeSurfer processing pipeline (version 6.0.1).¹⁷ Cortical thickness was averaged over both hemispheres using standard outputs of the FreeSurfer pipeline as described before.¹⁸ Relative brain volume was calculated by normalizing brain volume for estimated intracranial volume to account for variation in head size.¹⁹

Laboratory parameters

Routine laboratory parameters such as leucocytes, creatinine, sodium, potassium, glucose, glycated haemoglobin, and high-sensitivity C-reactive protein (hs-CRP) were immediately measured in fresh samples. Glomerular filtration rate (GFR) was calculated using the Chronic Kidney Disease Epidemiology Collaboration (CKD-EPI) formula for creatinine.²⁰

The following biomarkers were assayed in a blinded fashion using serum samples stored at -80°C in a dedicated biobank: (i) cardiac troponin I was measured using a high-sensitivity cardiac troponin I assay (ARCHITECT High Sensitive STAT Troponin I, Abbott Laboratories, Abbott Park, IL, USA) with a limit of detection of 1.9 ng/L;²¹ (ii) N-terminal pro-B-type natriuretic peptide (NT-proBNP) was measured using an immunoassay (Alere NT-proBNP for ARCHITECT, Abbott Diagnostics) with measurement ranges between 8.2 and 35 000 ng/L; and (iii) cystatin C was determined by the Abbott Cystatin C ARCHITECT c8000 assay with measurement ranges between 0.05 and 8.33 mg/L and a limit of detection of 0.05 mg/L. Coagulation parameters, including D-dimers, fibrinogen, prothrombin time according to Quick's method, as well as activated partial thromboplastin time, were measured in sodium citrated plasma samples stored at -80°C on a Atellica COAG 360 System analyzer (Siemens Healthineers, Erlangen, Germany) in a blinded fashion.

SARS-CoV-2 serology

For the detection of past SARS-CoV-2 infection and the qualitative serologic assay targeting the viral nucleocapsid protein, the Elecsys[®] Anti-SARS-CoV2 (Roche, Mannheim, Germany; analyzer: cobas e411) assay was used. To analyse neutralizing antibody responses, the quantitative assay Liaison[®] SARS-CoV-2 S1/S2 IgG (Diasorin, Saluggia, Italy; analyzer: Liaison XL) or the quantitative assay Elecsys[®] Anti-SARS-CoV-2 S (Roche; analyzer: cobas e411) were used. Quantitative values were normalized to the first World Health Organization standard for anti-spike antibodies (NIBSC code: 20/136; version 2.0, as of 17 December 2020) and presented as binding antibody unit (BAU)/mL [conversion factor 4.961 (Diasorin) and 0.9750 (Roche)]. All serological tests were performed according to the manufacturer's recommendations in an accredited laboratory (UKE Hamburg).

Cognitive function assessment

Mini-Mental State Examination (MMSE) was applied as a screening instrument for cognitive impairment and dementia.

Patient-related outcomes and quality-of-life assessment

Patient Health Questionnaire-9 and -15 (PHQ-9, PHQ-15), Generalized Anxiety Disorder Assessment (GAD-7), European Quality of Life 5 Dimensions (EQ-5D), as well as visual analogue scale (EQ-5D VAS) were assessed as central parameters of patient-reported outcomes (PRO).⁹

Main outcomes

Main outcomes per organ system were discussed and pre-defined among experts in a focus group to examine pre-defined hypotheses (Table 1).

Subgroup analyses

Subgroup analyses were performed to analyse potential differences between (i) severity of COVID-19 (asymptomatic or mild symptoms vs. moderate symptoms) and (ii) recruitment route of subjects with SARS-CoV-2 infection with respect to organ-specific main

outcomes. These analyses are explorative, given the resulting small sample sizes.

Statistics

Matching

The pool of possible controls was drawn from the cohort of the first 10 000 HCHS participants omitting seasonal effects and undetected COVID-19 infections. Matching was conducted using *k*-nearest neighbours without the re-use of controls and a variable ratio of cases and controls. Controls were matched for age at inclusion using a caliper of ± 2 years, dichotomized sex, the three categorical educational status according to the International Standard Classification of Education, and the availability of MRI examinations of the heart and the brain.²² More information on the setup and quality of the matching can be found in the [Supplementary material online](#). Matching groups were clustered by age, sex, and educational status of patients after SARS-CoV-2 infection leading to an *n:m* matching and more variability between clusters.

Imputation of missing data

Multivariate predictive mean imputation by chained equations with 100 imputations and 10 iterations was used to impute missing data.²³ Variables used for imputation included the matching cluster, age, sex, educational status as well as relevant comorbidities, and all variables used to analyse the hypotheses relevant to the medical speciality. Imputations were performed separately for patients after SARS-CoV-2 infection and controls as well as for each medical speciality. Information on specific handling of PRO can be found in the [Supplementary material online](#).

Statistical analysis

In the descriptive analysis, continuous data are presented as the median and interquartile range (IQR), and categorical data as absolute numbers and percentage.

Continuous outcomes were analysed using multiple linear mixed models, binary outcomes using multiple logistic mixed regression, both with matching cluster as random intercept. Regression results are presented as a forest plot depicting the comparison of patients after SARS-CoV-2 infection and controls. Regression estimates are provided, i.e. betas for continuous variables and odds ratios (OR) for binary outcomes. Parameters with skewed distributions were log-transformed before being entered into regression analyses, then re-transformed to enable interpretation. These parameters were left ventricular end-diastolic volume, high-sensitivity cardiac troponin I, NT-proBNP, leucocytes, and anti-spike antibodies.

P-values and 95% confidence intervals (CI) for pre-defined main outcomes were corrected for multiple testing within each organ system using the Bonferroni method.

All analyses were performed in R version 4.0.3.

Results

Baseline characteristics

The baseline characteristics of the 1771 participants are outlined in Table 2. The median age was 55 (IQR 51, 60) years in 443 subjects after SARS-CoV-2 infection vs. 57 (IQR 52, 62) years in 1328 matched controls. Female sex was present in 52.6 vs. 54.1%, respectively. Participants after SARS-CoV-2 infection and matched controls were comparable regarding socio-demographic characteristics, vital signs, anthropometry, patient history, and risk

Table 1 Main outcomes per organ system

Biological parameter	Corresponding surrogate
Respiratory system	
Lung volume	TLC in bodyplethysmography, % of predicted value
Airway function	sRaw in bodyplethysmography, % of predicted value
Cardiac system	
LV function	LVEF in TTE, %
RV function	TAPSE in TTE, mm
Focal myocardial fibrosis	Presence of late gadolinium enhancement on CMR
Myocardial damage	High-sensitivity cardiac troponin I, ng/L
Haemodynamic stress	NT-proBNP, ng/L
Vascular system	
Deep vein thrombosis	At least one non-compressible common femoral vein on venous ultrasound
Atherosclerosis	Presence of carotid plaques on carotid ultrasound
Renal system	
Renal function	GFR, mL/min/1.73 m ² Potassium, mmol/L
Metabolic and inflammatory system	
Metabolics	Glycated haemoglobin, %
Inflammation	High-sensitivity CRP, mg/L
Neurological system	
Vascular brain damage	Presence of cerebral micro bleeds on brain MRI Presence of infarct residuals on brain MRI
Brain atrophy	Relative brain volume, % Cortical thickness, mm
Neurocognition	
Screening for cognitive impairment	Mini-Mental State Examination
Psychosocial outcomes	
Severity of depression	PHQ-9
Generalized anxiety	GAD-7

Main outcomes selected by clinical relevance. CMR, cardiac magnetic resonance; CRP, C-reactive protein; GAD-7, Generalized Anxiety Disorder Assessment; GFR, glomerular filtration rate; LV, left ventricular; LVEF, left ventricular ejection fraction; MRI, magnetic resonance imaging; PHQ-9, Patient Health Questionnaire-9; RV, right ventricular; sRaw, specific airway resistance; TAPSE, tricuspid annular plane systolic excursion; TLC, total lung capacity; TTE, transthoracic echocardiogram.

Table 2 Baseline characteristics

	Subjects after SARS-CoV-2 infection (n = 443)	Matched controls (n = 1328)
Demographics		
Age, years	55 (51, 60)	57 (52, 62)
Female sex	233 (52.6)	719 (54.1)
Education ^a		
Low	90 (20.3)	329 (24.8)
Medium	88 (19.9)	289 (21.8)
High	265 (59.8)	710 (53.5)
Employment		
Full time	246 (56.4)	661 (51.8)
Part time	129 (29.6)	303 (23.7)
Unemployed	61 (14.0)	312 (24.5)
COVID-19-specific characteristics		
Self-reported disease severity at the time of infection [*]		
Asymptomatic	14 (3.2)	
Mild	253 (58.4)	
Moderate, no need for hospitalization	135 (31.2)	
Moderate, need for hospitalization, without ICU	31 (7.2)	
Detectable SARS-CoV-2 nucleocapsid antibody	411 (94.5)	
Neutralizing anti-spike antibodies, BAU/mL	189.83 (52.36, 536.21)	
Months between first positive SARS-CoV2 PCR test and study enrollment	9.58 (5.20, 10.60)	
Risk factors		
Hypertension	267 (61.5)	750 (58.6)
Diabetes mellitus	27 (6.4)	78 (6.3)
Dyslipidaemia	89 (20.9)	210 (16.8)
Smoking status		
Current	33 (7.5)	280 (21.2)
Former	163 (37.1)	556 (42.1)
Never	243 (55.4)	485 (36.7)
ESC score ^b	1.20 (0.60, 2.40)	1.20 (0.60, 2.40)
Vital signs and anthropometry		
Heart rate, b.p.m.	69 (61, 77)	68 (62, 76)
Systolic blood pressure, mmHg	137 (126, 150)	136 (125, 149)
Diastolic blood pressure, mmHg	87 (80, 94)	83 (76, 90)
BMI, kg/m ²	25.9 (23, 29)	25.7 (23.3, 29.0)
Medical history ^c		
Coronary artery disease	15 (3.4)	49 (3.8)
Myocardial infarction	7 (1.6)	24 (1.8)
Peripheral artery disease	13 (3.0)	24 (1.9)
Chronic kidney disease	49 (11.1)	126 (9.6)
Chronic lung disease	53 (12.0)	154 (11.8)
Neoplasia	43 (9.7)	151 (11.5)

Continuous variables are presented as median and interquartile range, and categorical variables are presented as absolute numbers and percentages.

Individuals after SARS-CoV-2 infection were mainly community patients as 93% were not hospitalized.

BAU, binding antibody unit; BMI, body mass index; ESC, European Society of Cardiology; ICU, intensive care unit; PCR, polymerase chain reaction.

^aEducational status defined according to the International Standard Classification of Education (ISCED).

^bESC score calculated for a 6-year risk of fatal cardiovascular disease.

^cSelf-reported.

*P-value for association of disease severity with anti-spike antibody concentration in linear regression <0.001.

factors. In total, 92.8% of participants after SARS-CoV-2 infection were managed as outpatients, reporting none (3.2%), mild (58.4%), or moderate (31.2%) symptoms at the time of SARS-CoV-2 infection. Hospitalization without need for intensive care support was required in only 7.2% of all participants in the post-SARS-CoV-2 cohort. Participants after SARS-CoV-2

infection were enrolled at a median of 9.6 months after the first positive PCR test. In 94.5% of patients after SARS-CoV-2 infection, SARS-CoV-2 nucleocapsid antibodies were detectable. In median, these patients had a neutralizing anti-spike antibody concentration of 190 BAU/mL (IQR 52, 536). Anti-spike antibody concentrations were associated with perceived symptom severity ($P < 0.001$, Table 2) as well as age ($P < 0.001$) and body mass index ($P = 0.033$) but none of the other baseline characteristics (see Supplementary material online, Table S4). Baseline characteristics stratified by disease severity and recruitment route can be found in Supplementary material online Tables S5 and S6.

Organ-specific outcome measures

Respiratory system

Total lung capacity was lower in post-SARS-CoV-2 cases compared with controls [99.1% of the predicted value vs. 102.4% of the predicted value, regression coefficient -3.24 (95% CI -5.57 , -0.91), adjusted $P = 0.014$]. At the same time, specific airway resistance, as assessed by sRaw, was significantly higher in patients after SARS-CoV-2 infection than matched controls [77.3% of the predicted value vs. 69.8% of the predicted value, regression coefficient 8.11 (95% CI 3.56, 12.65), adjusted $P = 0.001$, Table 3 and Figure 1].

Cardiac system

Left ventricular ejection fraction determined by both transthoracic echocardiography and cardiac MRI was numerically slightly decreased in patients after SARS-CoV-2 infection when compared with controls, while only the difference in left ventricular ejection fraction derived from transthoracic echocardiography remained statistically significant after adjustment for multiple testing [left ventricular ejection fraction on transthoracic echocardiography, 57.9 vs. 59.1%, regression coefficient -0.93 (95% CI -1.54 , -0.32), adjusted $P = 0.015$]. Measures of left ventricular diastolic function, assessed by E/e' and left atrial volume, were not increased in subjects after SARS-CoV-2 infection. Right ventricular systolic function, quantified by TAPSE using transthoracic echocardiography, was significantly reduced in patients after SARS-CoV-2 infection [TAPSE, 23.0 vs. 23.9 mm, regression coefficient -0.72 (95% CI -1.24 , -0.21), adjusted $P = 0.031$]. Additional right ventricular measures of systolic function such as right ventricular ejection fraction, assessed by cardiac MRI, and diastolic function such as peak tricuspid regurgitation velocity, showed no relevant intergroup changes.

There was a trend of more focal myocardial fibrosis, assessed by cardiac magnetic resonance LGE imaging, in participants after SARS-CoV-2 infection; however, LGE and myocardial T2 mapping (indicating myocardial oedema) did not differ significantly between patients after SARS-CoV-2 infection and matched controls. Furthermore, diffuse myocardial fibrosis was assessed by native myocardial T1 mapping and revealed comparable results in both groups, in particular participants after SARS-CoV-2 did not show any evidence for accelerated remodelling of the myocardium.

Both cardiac biomarkers, NT-proBNP [87.84 vs. 62.76 ng/L, multiplicative regression coefficient 1.41 (95% CI 1.29, 1.55), adjusted $P < 0.001$] and high-sensitivity cardiac troponin I [2.07 vs.

1.90 ng/L, multiplicative regression coefficient 1.14 (95% CI 1.05, 1.24), adjusted $P = 0.010$] were higher in patients after SARS-CoV-2 infection compared with matched controls. NT-proBNP concentrations ≥ 125 ng/L were more frequently observed in patients after SARS-CoV-2 infection than matched controls [33.2 vs. 18.2%, OR 2.39 (95% CI 1.82, 3.12), adjusted $P < 0.001$].

Whereas the corrected QTc interval was longer in patients after SARS-CoV-2 infection when compared with matched controls, no significant intergroup differences could be observed in further conduction abnormalities like PQ interval, QRS interval, atrioventricular blocks, or bundle branch blocks.

Vascular system

Sonographically non-compressible common femoral veins were found more frequently in participants after SARS-CoV-2 infection than in matched controls [43.2 vs. 22.2%, OR 2.68 (95% CI 1.77, 4.05), adjusted $P < 0.001$], independent of the side of measurement. Coagulation parameters did not differ between groups.

The mean CIMT assessed by carotid sonography was comparable between patients after SARS-CoV-2 infection and matched controls, but participants after SARS-CoV-2 infection more often presented atherosclerotic plaques [36.9 vs. 23.4%, OR 2.27 (95% CI 1.76, 2.93), adjusted $P < 0.001$]. In contrast, PSV was lower in participants after SARS-CoV-2 infection both in the ICA and CCA.

Renal system

Both markers of renal function, creatinine and cystatin C, were slightly elevated in patients after SARS-CoV-2 infection compared with matched controls. Ultimately, estimated GFR based on creatinine measurements was reduced in patients after SARS-CoV-2 infection by 2.35 mL/min/1.73 m² (95% CI -4.04 , -0.67 , adjusted $P = 0.019$). Similarly, serum levels of sodium and potassium were slightly decreased in post-SARS-CoV-2 cases [for potassium, 3.8 vs. 3.9 mmol/L, regression coefficient -0.12 (95% CI -0.15 , -0.09), adjusted $P < 0.001$].

Metabolic and inflammatory system

Whereas glucose concentrations were higher in patients after SARS-CoV-2 infection, glycated haemoglobin was similar in both groups [5.49 vs. 5.50%, regression coefficient -0.03 (95% CI -0.09 , 0.03), adjusted $P = 0.60$]. Despite only minimal numerical differences, hs-CRP concentrations [0.09 vs. 0.11 mg/L, regression coefficient -0.05 (95% CI -0.09 , -0.01), adjusted $P = 0.044$] were slightly lower in patients after SARS-CoV-2 infection.

Neurological system

Brain MRI was available in 188 post-SARS-CoV-2 cases and 483 matched controls. Numbers of cerebral microbleeds (3.7 vs. 4.5%, adjusted $P = 1.00$), infarct residuals (2.7 vs. 6.5%, adjusted $P = 0.27$), and stenoses of the intracerebral vessels (1.1 vs. 0.6%, $P = 0.34$) were comparable in patients after SARS-CoV-2 infection and matched controls. In quantitative analysis of brain structure, relative brain volume was comparable between groups [81.4 vs. 81.7%, regression coefficient -0.52 (95% CI -1.1 , 0.06), adjusted $P = 0.31$], while patients after SARS-CoV-2 infection had higher mean cortical thickness [2.65 vs. 2.63 mm, regression coefficient

Table 3 Descriptive distributions and regression outcomes by organ systems

Biological parameter	Corresponding surrogate	Subjects after SARS-CoV-2 infection (n = 443)	Matched controls (n = 1328)	Regression estimate ^a	Nominal P-value for regression estimates	Adjusted P-values	
Respiratory system							
Lung volume	TLC, % of predicted value	99.14 (90.37, 107.66)	102.48 (93.66, 112.03)	−3.24 (−5.57, −0.91)	0.0071	0.014	
	VC, % of predicted value	100.54 (90.88, 110.86)	104.67 (95.08, 115.16)	−4.43 (−6.97, −1.9)	<0.001		
	FVC, % of predicted value	99.48 (91.53, 107.13)	101.16 (90.79, 110.71)	−1.21 (−3.42, 1.01)	0.29		
	FRC, % of predicted value	105.39 (93.15, 119.83)	107.69 (94.87, 122.44)	−1.67 (−5.03, 1.69)	0.33		
Airway function	sRaw, % of predicted value	77.26 (58.89, 99.49)	69.76 (51.89, 91.85)	8.11 (3.56, 12.65)	<0.001	0.001	
	FEV ₁ , % of predicted value	98.35 (88.69, 107.17)	97.84 (87.55, 108.46)	0.05 (−2.26, 2.37)	0.97		
	FEV ₁ / FVC ratio	0.78 (0.74, 0.81)	0.77 (0.73, 0.80)	0.01 (0, 0.02)	0.083		
	Raw, % of predicted value	74.15 (58.39, 95.56)	69.26 (51.09, 93.67)	4.57 (−0.63, 9.76)	0.087		
Cardiac system							
TTE	LV function	57.88 (55.76, 60.27)	59.05 (55.46, 62.63)	−0.93 (−1.54, −0.32)	0.003	0.015	
	E/e' mean	6.66 (5.75, 7.74)	7.05 (6.03, 8.26)	−0.37 (−0.56, −0.18)	<0.001		
	TAPSE, mm	22.95 (20.37, 26.20)	23.88 (21.29, 26.79)	−0.72 (−1.24, −0.21)	0.006		
	TR Vmax, m/s	2.33 (2.12, 2.49)	2.29 (2.19, 2.49)	−0.04 (−0.1, 0.01)	0.14		
CMR	Focal myocardial fibrosis	40 (36.0)	67 (29.0)	1.39 (0.86, 2.27)	0.18	0.92	
	Diffuse myocardial fibrosis	1172 (1145, 1196)	1182 (1158, 1202)	−10.83 (−20.65, −1.02)	0.032		
Laboratory	Myocardial oedema	40 (38, 42)	40 (38, 42)	0.31 (−0.29, 0.92)	0.31	0.010 <0.001	
	LV function	68.11 (62.56, 72.97)	69.84 (64.93, 74.13)	−1.3 (−2.86, 0.26)	0.10		
	LV hypertrophy	64.92 (57.96, 71.59)	64.26 (55.18, 73.66)	0.91 (−1.65, 3.47)	0.49		
	LV volume	125.27 (106.51, 142.75) N	124.38 (106.78, 148.64)	0.99 (0.95, 1.04) ^b	0.82		
	Left atrium size	20.20 (15.95, 25.45)	18.76 (15.07, 24.19)	0.76 (−0.33, 1.85)	0.17		
	RV function	57.23 (51.27, 63.97)	57.79 (51.94, 63.94)	−0.72 (−2.44, 1.0)	0.41		
	Myocardial damage	High-sensitivity troponin I, ng/L	2.07 (1.30, 3.23)	1.90 (1.25, 2.88)	1.14 (1.05, 1.24) ^b		0.002
	Haemodynamic stress	NT-proBNP, ng/L	87.84 (55.65, 145.76)	62.76 (38.18, 106.39)	1.41 (1.29, 1.55) ^b		<0.001
ECG	Arrhythmia	13 (3.0)	45 (3.4)	0.94 (0.5, 1.77)	0.84	0.070	
	Conduction	160.84 (146.00, 179.33)	158.91 (145.74, 176.39)	2.68 (−0.22, 5.57)	0.67		
	disturbances	93.00 (85.61, 101.00)	92.00 (86.00, 99.69)	0.31 (−1.12, 1.74)	0.67		
		433.90 (414.39, 454.88)	429.64 (413.16, 444.91)	6.47 (3.57, 9.37)	<0.001		
Symptoms	AV blocks	33 (7.5)	67 (5.1)	1.51 (0.98, 2.33)	0.064	0.28	
	Bundle branch blocks	41 (9.3)	104 (7.8)	1.24 (0.84, 1.83)	0.28		
	NYHA class						
	I	392 (88.5)	1211 (91.2)	Reference ^c		0.69	
	II	27 (6.1)	77 (5.8)	1.1 (0.68, 1.79)			
	III or IV	24 (5.4)	41 (3.1)	1.87 (1.06, 3.23)	0.032		

Continued

Table 3 Continued

Biological parameter	Corresponding surrogate	Subjects after SARS-CoV-2 infection (n = 443)	Matched controls (n = 1328)	Regression estimate ^a	Nominal P-value for regression estimates	Adjusted P-values
<i>Vascular system</i>						
Veins	Deep vein thrombosis	At least one non-compressible common femoral vein	99 (43.2)	49 (22.2)	2.68 (1.77, 4.05)	<0.001
		Non-compressible common femoral vein right	70 (30.6)	28 (12.7)	3.06 (1.87, 4.99)	<0.001
		Non-compressible deep femoral vein left	69 (30.1)	29 (13.1)	2.86 (1.76, 4.62)	<0.001
Arteries	Atherosclerosis	Carotid intima-media thickness, mm	0.70 (0.62, 0.79)	0.71 (0.63, 0.81)	-0.01 (-0.02, 0.01)	0.35
		Carotid plaques	164 (36.9)	311 (23.4)	2.27 (1.76, 2.93)	<0.001
Laboratory		Peak systolic velocity CCA, m/s	0.80 (0.71, 0.90)	0.86 (0.75, 0.99)	-0.07 (-0.09, -0.06)	<0.001
		Peak systolic velocity ICA, m/s	0.64 (0.56, 0.75)	0.72 (0.62, 0.83)	-0.07 (-0.09, -0.05)	<0.001
		D-dimer, µg/L	0.24 (0.19, 0.37)	0.29 (0.20, 0.42)	-0.08 (-0.3, 0.14)	0.460
		Fibrinogen, g/L	2.47 (2.06, 2.87)	2.41 (1.99, 2.78)	0.06 (-0.23, 0.35)	0.700
		Quick prothrombin time, %	85.59 (75.59, 94.20)	79.89 (71.45, 87.31)	3.75 (-5.11, 12.62)	0.410
		Activated partial thromboplastin time, s	34.59 (31.51, 38.12)	35.70 (33.08, 38.62)	-0.49 (-4.04, 3.05)	0.790
		GFR, mL/min/1.73 m ²	108.89 (86.22, 120.70)	109.14 (89.21, 120.44)	-2.35 (-4.04, -0.67)	0.006
<i>Renal system</i>						
Renal function		Creatinine, mg/dL	0.80 (0.73, 0.88)	0.78 (0.72, 0.86)	0.02 (0.01, 0.04)	0.002
		Cystatin C, mg/L	0.97 (0.87, 1.07)	0.96 (0.86, 1.05)	0.02 (0, 0.03)	0.033
		Potassium, nmol/L	3.8 (3.6, 3.9)	3.9 (3.7, 4.0)	-0.12 (-0.15, -0.09)	<0.001
		Sodium, mmol/L	139 (138, 140)	139 (138, 141)	-0.28 (-0.5, -0.05)	0.016
<i>Metabolic and inflammatory system</i>						
Metabolics		HbA1c, %	5.49 (5.30, 5.61)	5.50 (5.30, 5.70)	-0.03 (-0.09, 0.03)	0.30
		Glucose, mg/dL	94.45 (88.02, 102.00)	90.98 (85.00, 98.00)	3.89 (1.9, 5.87)	<0.001
Inflammation		High-sensitivity CRP, mg/L	0.09 (0.05, 0.19)	0.11 (0.06, 0.26)	-0.05 (-0.09, -0.01)	0.022
		Leucocyte, count per µL	5.57 (4.71, 6.41)	5.90 (4.89, 7.10)	0.94 (0.91, 0.97) ^b	<0.001
<i>Neurological system</i>						
Vascular brain damage		Cerebral microbleeds	7 (3.72)	21 (4.45)	0.86 (0.35, 2.1)	0.74
		Infarct residuals	5 (2.66)	31 (6.49)	0.4 (0.15, 1.07)	0.068
		Intracerebral stenoses	2 (1.1)	3 (0.63)	2.72 (0.35, 21.14)	0.34
Brain atrophy		Relative brain volume, %	81.37 (78.88, 83.70)	81.69 (78.90, 83.85)	-0.52 (-1.1, 0.06)	0.077
		Cortical thickness, mm	2.65 (2.60, 2.72)	2.63 (2.57, 2.69)	0.03 (0.01, 0.05)	<0.001
<i>Neurocognition</i>						
Screening for cognitive impairment		Mini-Mental State Examination	29 (28, 29)	28 (27, 29)	0.26 (0.1, 0.42)	0.002
<i>Psychosocial outcomes</i>						

Continued

Table 3 Continued

Biological parameter	Corresponding surrogate	Subjects after SARS-CoV-2 infection (n = 443)	Matched controls (n = 1328)	Regression estimate ^a	Nominal P-value for regression estimates	Adjusted P-values
Severity of depression	PHQ-9	3 (1, 6)	3 (1, 6)	0.34 (−0.06, 0.74)	0.10	0.20
Severity of somatic symptoms	PHQ-15	4 (2, 7)	4.00 (2, 7)	0.21 (−0.23, 0.64)	0.35	
Generalized anxiety	GAD-7	2 (0, 5.00)	2 (1, 4)	0 (−0.35, 0.35)	0.99	1.00
Quality of life	EQ-5D: index	0.91 (0.87, 1.00)	0.91 (0.89, 1.00)	0 (−0.01, 0.01)	0.75	
	EQ-5D: VAS	81 (75, 90)	82 (75, 90)	−1.5 (−3.23, 0.23)	0.090	

Continuous variables are presented as median and interquartile range, and categorical variables are presented as absolute numbers and percentages. AV, atrioventricular; CCA, common carotid artery; CMR, cardiac magnetic resonance; CRP, C-reactive protein; ECG, electrocardiogram; EQ-5D, European Quality of Life 5 Dimensions visual analogue scale; FEV₁, forced expiratory volume in 1 s; FRC, functional residual capacity; FVC, forced vital capacity; GAD-7, Generalized Anxiety Disorder Assessment; GFR, glomerular filtration rate; HbA1c, glycated haemoglobin; ICA, internal carotid artery; LAVI, left atrial volume indexed to body surface area; LV, left ventricular; LVEDV, left ventricular end-diastolic volume; LVEF, left ventricular ejection fraction; NT-proBNP, N-terminal pro-B-type natriuretic peptide; NYHA, New York Heart Association; PHQ-9, Patient Health Questionnaire-9; PHQ-15, Patient Health Questionnaire-15; Raw, airway resistance; RVEF, right ventricular ejection fraction; sRaw, specific airway resistance; TAPSE, tricuspid annular plane systolic excursion; TLC, total lung capacity; TR Vmax, peak tricuspid regurgitation velocity; TTE, transthoracic echocardiogram; VC, vital capacity. ^aRegression estimates for patients after SARS-CoV-2 infection vs. matched controls. Regression estimates are presented as beta and 95% confidence interval for continuous variables and odd ratios and 95% confidence interval for categorical variables. ^bRegression estimates are presented as beta for retransformed logarithmic outcomes. Betas are multiplicative instead of additive. ^cNYHA Class II, III, and IV compared with NYHA Class I in binary logistic regression.

0.03 (95% CI 0.01, 0.05), adjusted $P = 0.002$] when compared with matched controls.

Neurocognitive testing

The median score in MMSE was higher in patients after SARS-CoV-2 infection than in matched controls [29 vs. 28, regression coefficient 0.26 (95% CI 0.1, 0.42), adjusted $P = 0.002$].

Quality of life and psychosocial outcomes

There were no significant differences between patients after SARS-CoV-2 infection and matched controls in terms of quality of life, severity of depression, severity of somatic symptom, or generalized anxiety.

Associations of antibody concentration with main outcomes

Associations of anti-spike antibody concentration with main outcomes across the various organ systems can be found in [Supplementary material online, Table S7](#). In brief, no systematic associations could be observed except for a direct association between antibody concentrations and infarct residuals on brain MRI.

Subgroup analyses

Within the subjects with prior SARS-CoV-2 infection, no systematic differences in organ-specific outcomes could be observed when comparing mild vs. moderate course of COVID-19 as well as recruitment route, except for higher levels of anxiety and depression in subjects with the moderate course of COVID-19 compared with subjects with a milder course (see [Supplementary material online, Tables S8 and S9](#)).

Discussion

In more than 1700 individuals, we extensively phenotyped multi-organ-specific structure and function and explored neurocognitive and PRO to comprehensively assess the intermediate to long-term effects of mild and moderate COVID-19 disease. We consistently observed organ-specific subclinical involvement ([Graphical Abstract](#)).

Autopsy studies indicate that SARS-CoV-2 affects multiple organs beyond the respiratory tract, including the heart, brain, and kidneys.^{6,24} Some patients continue to suffer from heterogeneous symptoms after the acute phase of critical illness. These conditions are described as ‘post-COVID-19 syndrome’ or—if symptoms continue longer than 6 months—as ‘long COVID-19 syndrome’. Clinical, imaging, or laboratory findings should accompany the diagnosis of post- or long COVID-19.²⁵ To date, longer term effects after a mild to moderate COVID-19 disease course remain largely unknown. A systematic and comprehensive exploration of potential multi-organ impairment is important to plan surveillance and potential diagnostic testing after recovery.

While there is evidence that post-COVID-19 patients with mild to moderate disease have preserved lung volumes,²⁶ we found a significantly lower TLC in subjects after mild to moderate infection compared with controls. This is in line with previous findings of a reduction in TLC beginning after mild COVID-19.²⁷ Residual

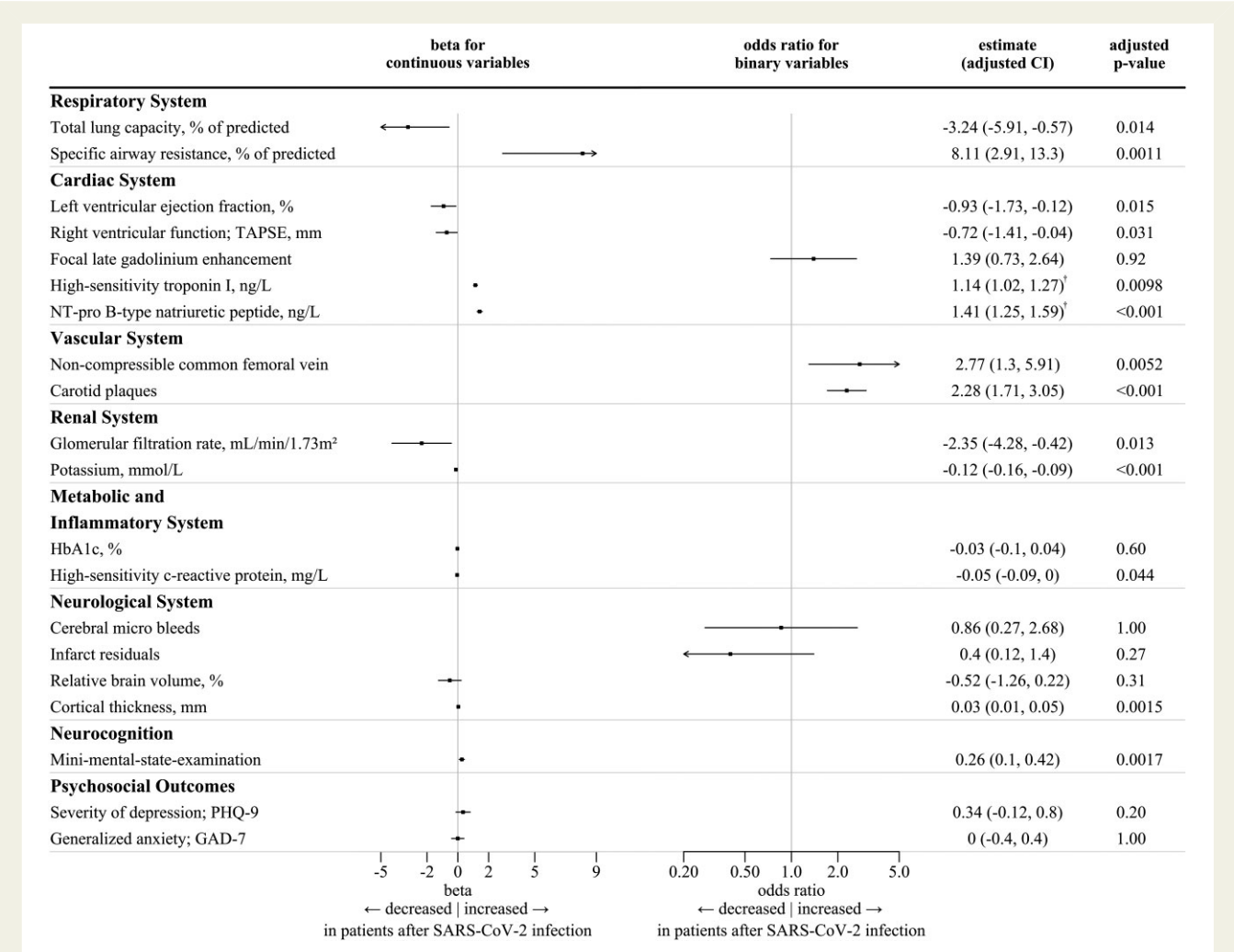


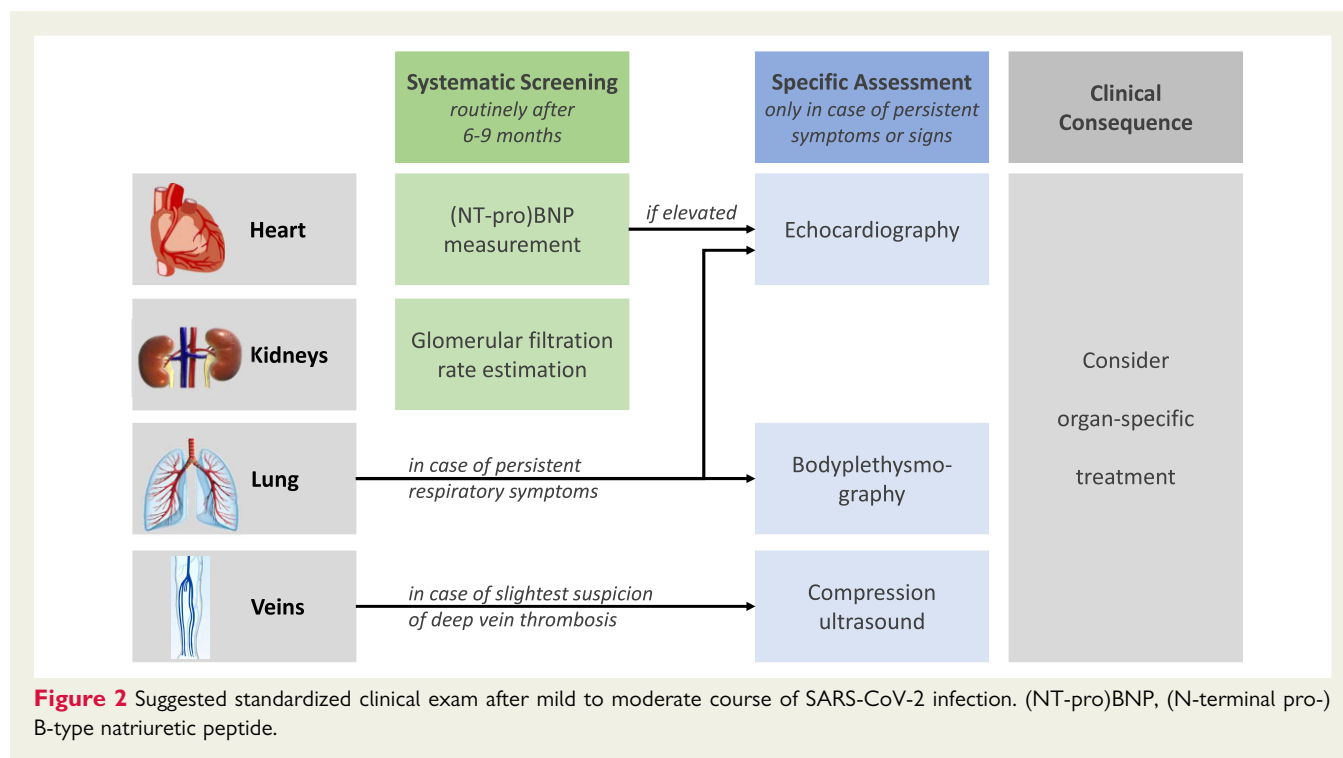
Figure 1 Forest plot depicting the association of prior SARS-CoV-2 infection with organ-specific main outcomes. Regression estimates for patients after SARS-CoV-2 infection vs. matched controls. Regression estimates are presented as beta and 95% confidence interval for continuous variables and odd ratios and 95% confidence interval for categorical variables. P-values are adjusted using the Bonferroni correction for main outcomes within each organ system. [†]Regression estimates are presented as beta for retransformed logarithmic outcomes. Betas are multiplicative instead of additive. GAD-7, Generalized Anxiety Disorder Assessment; HbA1c, glycated haemoglobin; NT-proBNP, N-terminal pro-B-type natriuretic peptide; PHQ-9, Patient Health Questionnaire-9; TAPSE, tricuspid annular plane systolic excursion.

inflammatory processes or beginning subclinical fibrotic remodeling might explain the slightly lower lung volumes observed in the post-SARS-CoV-2 cohort.²⁸ Congruent with histological findings, we found higher specific airway resistance in participants after SARS-CoV-2 infection.²⁹ Assessment of lung function should be considered after recovery from COVID-19 at slightest suspicion even in apparently healthy individuals (Figure 2).

From a cardiovascular perspective, a numerically small reduction of left ventricular ejection fraction with 1–2% difference was observed in participants after SARS-CoV-2 infection accompanied by higher concentration of cardiac biomarkers reflecting modest myocardial involvement. In a very long-term perspective, even a small reduction of left ventricular function and a slight increase in NT-proBNP concentration translate into an increased risk of mortality in the general population.^{30,31} Therefore, the determination of NT-proBNP, followed by echocardiography

control in the case of elevated concentrations, may be recommended after COVID-19 recovery to avoid untreated dysfunction of the heart.

Most importantly, our data suggest a significantly higher prevalence of deep venous thrombosis in participants after SARS-CoV-2 infection. Although affected by certain examiner bias, compression ultrasound is commonly accepted and widely used as the reference standard in everyday clinical practice.³² The present findings extend the rapidly increasing evidence for an association between COVID-19 and venous thromboembolism,^{4,33} while adding a prospectively enrolled cohort with mild or moderate disease. Of note, levels of coagulation parameters assessed at a median of 9.6 months after mild to moderate SARS-CoV-2 infection did not differ when compared with matched controls. Therefore, we may assume that acute thrombotic events themselves, associated with activation of the coagulation



and fibrinolytic cascade, occurred much earlier during the course of COVID-19. In this context, the non-compressible veins observed in our study are to be interpreted as remnants of the fibrotic processes replacing prior thrombotic material. Considering the existing evidence, the current study results suggest that a guideline-based surveillance with active screening for deep vein thrombosis in the case of minimal clinical suspicion early during COVID-19 infection should be considered.³²

The assessment of the arterial system indicated more frequent carotid plaques in post-SARS-CoV-2 participants compared with matched controls, while CIMT was comparable between groups. Whether this finding may be fully explained by the higher susceptibility of patients with the prevalent atherosclerotic disease for COVID-19^{34,35} or to some extent also by common immunological pathways involved in SARS-CoV-2 infections and atherosclerosis³⁶ needs to be addressed in future longitudinal studies. Lower peak systolic flow velocities in the carotid arteries in patients after SARS-CoV-2 infection are in line with the trend towards a lower ejection fraction and presence of carotid plaques, as these parameters were reported to be associated recently.¹⁶

Individuals after SARS-CoV-2 recovery were also found to have a subtle decrease in kidney function compared with the matched controls, which also does not appear clinically relevant at the time of investigation. However, autopsy studies have shown a distinct renal tropism related to SARS-CoV-2 and early urine abnormalities associated with mortality as well as multi-organ failure in hospitalized COVID-19.⁶ The differences observed in our study might thus reflect a specific SARS-CoV-2-related injury with a starting trajectory to early chronic kidney disease, being an important risk factor for mortality and cardiovascular events.³⁷

Therefore, we argue for a follow-up assessment of a renal function marker 6–9 months even after mild SARS-CoV-2 infections.

Brain MRI was available in a large subgroup of patients and did not reveal any signs of increased vascular brain damage. The presence and number of cerebral microbleeds and white matter hyperintensities as the most common hallmark of cerebral small vessel disease were comparable between participants recovered from mild to moderate COVID-19 and controls. This contrasts with findings in cohorts of severely ill COVID-19 patients, for whom both white matter lesions and microhaemorrhages have been reported.³⁸ The presence of vascular brain damage may thus be a phenomenon that is only observed in the severe course of COVID-19. Quantitative analysis of structural brain MRI did not show signs of overall brain atrophy, as relative brain volume was comparable between groups, and even showed a higher mean cortical thickness in patients after SARS-CoV-2 infection. This, again, is in contrast to a recent longitudinal analysis of brain imaging from participants of the UK Biobank who recovered from COVID-19, which showed brain atrophy and a regional reduction in grey matter thickness.³⁹ We also did not find any sign of cognitive impairment in patients after mild to moderate COVID-19. This adds to recent reports of persistent impaired cognitive function in few individuals who recovered from severe COVID-19.⁴⁰

Central parameters of PRO like depression, anxiety, and quality of life were tested. In none of the five scales, significant differences were observed in the main analysis. However, in an explorative subgroup analysis, higher degrees of depression and anxiety were observed in subjects with moderate course of COVID-19 when compared with subjects with none or only mild symptoms. These findings extend and corroborate previous work describing serious long-COVID-19 symptoms after intensive care courses

of COVID-19, which also affect the psychosocial domain.⁴¹ Individuals after mild to moderate disease might have normalized their previously elevated levels of anxiety and depression by the time of the survey.

The following limitations merit consideration. In this study, cases were only assessed after exposure to SARS-CoV-2. As assessment was not available prior to SARS-CoV-2 infection, multi-organ functions were compared with matched controls from the general population without exposure. Accordingly, as this is a cross-sectional study, we cannot infer on future developments and causality, but suggest that these findings represent signs of subtle medium to long-term multi-organ affection persisting after recovery from mild to moderate COVID-19, where most cases were not hospitalized.

Also, a selection bias might have occurred in the post-SARS-CoV-2 group of this study as the public invitation resulted in the participation of highly motivated post-SARS-CoV-2 study individuals, which particularly might have led to better performance in neurocognitive tests and quality-of-life questionnaires. However, the versatile multi-organ assessment consistently describes multi-organ affection even in the case of selection bias towards healthier or more motivated post-SARS-CoV-2 study individuals. As pharmacological COVID-19 therapies were not assessed in this study, we cannot quantify their impact on multi-organ function. However, given the high proportion of individuals with only mild symptoms and outpatient management in this data set, no relevant impact on reported outcomes is assumed. In addition, hs-CRP levels were very low and comparable in both groups. As levels were below the limit of detection at 0.1 mg/dL in about half of the populations, we may not comment on hypothetical very small differences in the extremely low end. Lastly, data on outcome variables were not completely available in all subjects. Multiple imputation was used to at least partly correct for this aspect.

Particular study strengths exist. The entire study population had been evaluated by one of the most comprehensive study protocols ever applied to evaluate multi-organ function, neurocognition, and PRO in patients recovered from mild to moderate COVID-19 within the frame of the HCHS. Participants after mild to moderate COVID-19 qualified with at least one positive PCR test. Further, antibody status was obtained. Finally, matched controls had been randomly recruited from the same geographic region via registration office within the frame of the HCHS.

Given that moderate SARS-CoV-2 infection may impact multi-organ function in the longer term, comprehensive preventive strategies such as hygiene measures, social distancing, and vaccination seem crucial.

In conclusion, in the HCHS COVID project, we demonstrate that patients who apparently recovered from mild to moderate COVID-19 suffer from modest subclinical multi-organ affection related to thrombotic, pulmonary, cardiac, and renal function without signs of structural brain damage, obvious impairment in cognitive function, or quality of life. Whereas the impact on very long-term outcome remains unclear, a standardized clinical exam of these conditions after recovery is recommended.

Data availability

The data underlying this article will be shared on reasonable request to the corresponding author.

Acknowledgements

The authors acknowledge the participants of the Hamburg City Health Study, the staff at the Epidemiological Study Center, the Hamburg City Health Study research consortium and steering board committee, as well as its cooperation partners, and patrons.

Funding

This project was specifically supported by Senat und Behörde für Wissenschaft, Forschung, Gleichstellung und Bezirke (BWFG) (Reference E43026-03.HCHS); Hamburg and the Deutsche Forschungsgemeinschaft (Grant Number TH1106/5-1; AA93/2-1). The HCHS is generally funded by the euCanSHare grant agreement (Grant Number 825903-euCanSHare H2020); the Foundation Leducq (Grant Number 16 CVD 03); and the Innovative medicine initiative (Grant Number 116074). The HCHS is additionally supported by Deutsche Gesetzliche Unfallversicherung (DGUV); Deutsches Krebsforschungszentrum (DKFZ); Deutsches Zentrum für Herz-Kreislauf-Forschung (DZHK); Deutsche Stiftung für Herzforschung; Seefried Stiftung; Amgen; Bayer; Novartis; Schiller; Siemens; Topcon; and Unilever. The study is further supported by donations from the 'Förderverein zur Förderung der HCHS e.V.', and TePe® (2014). Sponsor funding has in no way influenced the content or management of this study.

Conflict of interest: C.S.-L. reports funding from the City of Hamburg, S.B. reports institution funding from Bayer, Siemens, Novartis, and the City of Hamburg. We acknowledge support to TZ from the German Centre for Cardiovascular Research (FKZ 81Z1710101 and FKZ 81Z0710102).

Supplementary material

Supplementary material is available at *European Heart Journal* online.

References

1. World Health Organization. Weekly epidemiological update on COVID-19. <https://www.who.int/publications/m/item/weekly-epidemiological-update-on-covid-19-28-december-2021>
2. Robert Koch Institut. Wöchentlicher Lagebericht des RKI zur Coronavirus-Krankheit-2019 (COVID-19). https://www.rki.de/DE/Content/InfAZ/N/Neuartiges_Coronavirus/Situationsberichte/Wochenbericht/Wochenbericht_2021-11-18.pdf?__blob=publicationFile
3. Tolksdorf K, Buda S, Schuler E, Wieler LH, Haas W. Eine höhere Letalität und lange Beatmungsdauer unterscheiden COVID-19 von schwer verlaufenden Atemwegsinfektionen in Grippewellen. *Epidemiol Bull* 2020;**41**:3–10.
4. Edler C, Schröder AS, Aepfelbacher M, Fitzek A, Heinemann A, Heinrich F, et al. Dying with SARS-CoV-2 infection—an autopsy study of the first consecutive 80 cases in Hamburg, Germany. *Int J Legal Med* 2020;**134**:1275–1284.
5. Tan BK, Mainbourg S, Friggeri A, Bertolotti L, Douplat M, Dargaud Y, et al. Arterial and venous thromboembolism in COVID-19: a study-level meta-analysis. *Thorax* 2021;**76**:970–979.
6. Puelles VG, Lütgehetmann M, Lindenmeyer MT, Sperhake JP, Wong MN, Allweiss L, et al. Multiorgan and renal tropism of SARS-CoV-2. *N Engl J Med* 2020;**383**:590–592.
7. Ellul MA, Benjamin L, Singh B, Lant S, Michael BD, Easton A, et al. Neurological associations of COVID-19. *Lancet Neurol* 2020;**19**:767–783.
8. Huang C, Huang L, Wang Y, Li X, Ren L, Gu X, et al. 6-month consequences of COVID-19 in patients discharged from hospital: a cohort study. *Lancet* 2021;**397**:220–232.
9. Jagodzinski A, Johansen C, Koch-Gromos U, Aarabi G, Adam G, Anders S, et al. Rationale and design of the Hamburg City Health Study. *Eur J Epidemiol* 2020;**35**:169–181.
10. Miller MR, Hankinson J, Brusasco V, Burgos F, Casaburi R, Coates A, et al. Standardisation of spirometry. *Eur Respir J* 2005;**26**:319–338.

11. Wanger J, Clausen JL, Coates A, Pedersen OF, Brusasco V, Burgos F, et al. Standardisation of the measurement of lung volumes. *Eur Respir J* 2005;**26**: 511–522.
12. Wenzel J-P, Petersen E, Nikorowitsch J, Muller J, Kölbel T, Reichenspurner H, et al. Aortic root dimensions as a correlate for aortic regurgitation's severity. *Int J Cardiovasc Imaging* 2021;**37**:3439–3449.
13. Schulz-Menger J, Bluemke DA, Bremerich J, Flamm SD, Fogel MA, Friedrich MG, et al. Standardized image interpretation and post-processing in cardiovascular magnetic resonance - 2020 update: Society for Cardiovascular Magnetic Resonance (SCMR): Board of Trustees Task Force on Standardized Post-Processing. *J Cardiovasc Magn Reson* 2020;**22**:19.
14. Bohnen S, Awanosov M, Jagodzinski A, Schnabel RB, Zeller T, Karakas M, et al. Cardiovascular magnetic resonance imaging in the prospective, population-based, Hamburg City Health cohort study: objectives and design. *J Cardiovasc Magn Reson* 2018;**20**:68.
15. Messroghli DR, Moon JC, Ferreira VM, Grosse-Wortmann L, He T, Kellman P, et al. Clinical recommendations for cardiovascular magnetic resonance mapping of T1, T2, T2* and extracellular volume: a consensus statement by the Society for Cardiovascular Magnetic Resonance (SCMR) endorsed by the European Association for Cardiovascular Imaging (EACVI). *J Cardiovasc Magn Reson* 2017;**19**:75.
16. Rimmle DL, Borof K, Wenzel J-P, Jensen M, Behrendt C-A, Waldeyer C, et al. Differential association of flow velocities in the carotid artery with plaques, intima media thickness and cardiac function. *Atherosclerosis Plus* 2021;**43**:18–23.
17. Fischl B. FreeSurfer. *Neuroimage* 2012;**62**:774–781.
18. Cheng B, Dietzmann P, Schulz R, Boenstrup M, Krawinkel L, Fiehler J, et al. Cortical atrophy and transcallosal diaschisis following isolated subcortical stroke. *J Cereb Blood Flow Metab* 2020;**40**:611–621.
19. Malone IB, Leung KK, Clegg S, Barnes J, Whitwell JL, Ashburner J, et al. Accurate automatic estimation of total intracranial volume: a nuisance variable with less nuisance. *Neuroimage* 2015;**104**:366–372.
20. Levey AS, Stevens LA, Schmid CH, Zhang YL, Castro AF, 3rd, Feldman HI, et al. A new equation to estimate glomerular filtration rate. *Ann Intern Med* 2009;**150**: 604–612.
21. Apple FS, Ler R, Murakami MM. Determination of 19 cardiac troponin I and T assay 99th percentile values from a common presumably healthy population. *Clin Chem* 2012;**58**:1574–1581.
22. UNESCO Institute for Statistics. *International Standard Classification of Education ISCED 2011*. Montreal: UIS; 2012. p. 85.
23. van Buuren S, Groothuis-Oudshoorn K. mice: Multivariate Imputation by Chained Equations in R. *J Stat Softw* 2011;**45**:67.
24. Basso C, Leone O, Rizzo S, De Gaspari M, van der Wal AC, Aubry M-C, et al. Pathological features of COVID-19-associated myocardial injury: a multicentre cardiovascular pathology study. *Eur Heart J* 2020;**41**:3827–3835.
25. Yan Z, Yang M, Lai C-L. Long COVID-19 syndrome: a comprehensive review of its effect on various organ systems and recommendation on rehabilitation plans. *Biomedicine* 2021;**9**:966.
26. Lombardi F, Calabrese A, Iovene B, Pierandrei C, Lerede M, Varone F, et al. Residual respiratory impairment after COVID-19 pneumonia. *BMC Pulm Med* 2021;**21**:241.
27. Mo X, Jian W, Su Z, Chen M, Peng H, Peng P, et al. Abnormal pulmonary function in COVID-19 patients at time of hospital discharge. *Eur Respir J* 2020;**55**:2001217.
28. Gattinoni L, Chiumello D, Caironi P, Busana M, Romitti F, Brazzi L, et al. COVID-19 pneumonia: different respiratory treatments for different phenotypes? *Intensive Care Med* 2020;**46**:1099–1102.
29. Carsana L, Sonzogni A, Nasr A, Rossi RS, Pellegrinelli A, Zerbi P, et al. Pulmonary post-mortem findings in a series of COVID-19 cases from northern Italy: a two-centre descriptive study. *Lancet Infect Dis* 2020;**20**:1135–1140.
30. Wang TJ, Evans JC, Benjamin EJ, Levy D, LeRoy EC, Vasan RS. Natural history of asymptomatic left ventricular systolic dysfunction in the community. *Circulation* 2003;**108**:977–982.
31. Di Castelnuovo A, Veronesi G, Costanzo S, Zeller T, Schnabel RB, de Curtis A, et al. NT-proBNP (N-terminal pro-B-type natriuretic peptide) and the risk of stroke. *Stroke* 2019;**50**:610–617.
32. Kakkos SK, Gohel M, Baekgaard N, Bauersachs R, Bellmunt-Montoya S, Black SA, et al. Editor's Choice - European Society for Vascular Surgery (ESVS) 2021 clinical practice guidelines on the management of venous thrombosis. *Eur J Vasc Endovasc Surg* 2021;**61**:9–82.
33. Tan BK, Mainbourg S, Friggeri A, Bertoletti L, Douplat M, Dargaud Y, et al. Arterial and venous thromboembolism in COVID-19: a study-level meta-analysis. *Thorax* 2021;**76**:970–979.
34. Task Force for the management of COVID-19 of the European Society of Cardiology, Baigent C, Windecker S, Andreini D, Arbelo E, Barbato E, et al. European Society of Cardiology guidance for the diagnosis and management of cardiovascular disease during the COVID-19 pandemic: part 1—epidemiology, pathophysiology, and diagnosis. *Eur Heart J* 2022;**43**:1033–1058.
35. Baigent C, Windecker S, Andreini D, Arbelo E, Barbato E, Bartorelli AL, et al. ESC guidance for the diagnosis and management of cardiovascular disease during the COVID-19 pandemic: part 2—care pathways, treatment, and follow-up. *Eur Heart J* 2022;**43**:1059–1103.
36. Sagris M, Theofilis P, Antonopoulos AS, Tsioufis C, Oikonomou E, Antoniadou C, et al. Inflammatory mechanisms in COVID-19 and atherosclerosis: current pharmaceutical perspectives. *Int J Mol Sci* 2021;**22**:6607.
37. Manjunath G, Tighiouart H, Ibrahim H, MacLeod B, Salem DN, Griffith JL, et al. Level of kidney function as a risk factor for atherosclerotic cardiovascular outcomes in the community. *J Am Coll Cardiol* 2003;**41**:47–55.
38. Kremer S, Lersy F, de Sèze J, Ferrè JC, Maamar A, Carsin-Nicol B, et al. Brain MRI findings in severe COVID-19: a retrospective observational study. *Radiology* 2020;**297**:E242–E251.
39. Douaud G, Lee S, Alfaro-Almagro F, Arthofer C, Wang C, Lange F, et al. Brain imaging before and after COVID-19 in UK Biobank. *medRxiv* 2021. doi:10.1101/2021.06.11.21258690
40. Graham EL, Clark JR, Orban ZS, Lim PH, Szymanski AL, Taylor C, et al. Persistent neurologic symptoms and cognitive dysfunction in non-hospitalized Covid-19 "long haulers". *Ann Clin Transl Neurol* 2021;**8**:1073–1085.
41. Taboada M, Cariñena A, Moreno E, Rodríguez N, Domínguez MJ, Casal A, et al. Post-COVID-19 functional status six-months after hospitalization. *J Infect* 2021;**82**:e31–e33.